Journal of Materials Chemistry C

Accepted Manuscript

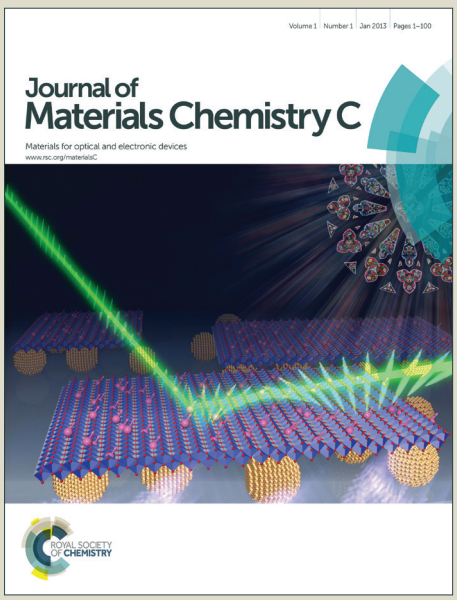

This is an *Accepted Manuscript*, which has been through the Royal Society of Chemistry peer review process and has been accepted for publication.

Accepted Manuscripts are published online shortly after acceptance, before technical editing, formatting and proof reading. Using this free service, authors can make their results available to the community, in citable form, before we publish the edited article. We will replace this *Accepted Manuscript* with the edited and formatted *Advance Article* as soon as it is available.

You can find more information about *Accepted Manuscripts* in the Information for Authors.

Please note that technical editing may introduce minor changes to the text and/or graphics, which may alter content. The journal's standard Terms & Conditions and the Ethical guidelines still apply. In no event shall the Royal Society of Chemistry be held responsible for any errors or omissions in this *Accepted Manuscript* or any consequences arising from the use of any information it contains.

ROYAL SOCIETY OF CHEMISTRY

www.rsc.org/materialsC

Journal Name

RSCPublishing

ARTICLE

Structural, mesomorphic, photoluminescent and thermoelectric studies of mononuclear and polymeric complexes of copper(II) with 2-hexyldecanoato and 4,4'-bipyridine ligands

Cite this: DOI: 10.1039/xoxxoooooox

Received ooth January 2012,
Accepted ooth January 2012

DOI: 10.1039/xoxxoooooox

www.rsc.org/

Norbani Abdullah,*[a] Rauzah Hashim,[a] Lailatun Nazirah Ozair,[a] Yasameen Al-Hakem,[a] Habibah Samsudin,[a] Anita Marlina,[a] Malinda Salim,[a] Suhana Mohd. Said,[b] Balamurugan Subramanian,[b] Abdul Rahman Nordin[b]

$[Cu(R)_2(bpy)_2].2RH$ (**1**) and $[Cu_2(R)_4(bpy)]_x$ (**2**) were obtained from the reaction of $[Cu_2(R)_4(RH)_2]$ (R = 2-hexyldecanoato) with 4,4'-bipyridine (bpy) under different work-up procedures. Complex **1** was single crystals and its molecular structure showed a distorted octahedral Cu(II) with two chelating bidentate R. Complex **2** has similar structure as crystals of a linear-chain coordination polymer, $[Cu_2(CH_3(CH_2)_5COO)_4(bpy)]_x$ (**3**). Both **1** and **2** were thermally stable (T_{dec} = 240 °C for **1**; 220 °C for **2**), have low melting temperatures (T_m = 52.3 °C for **1**; T_m = 48.3 °C for **2**) and exhibited temperature-dependent mesomorphisms. For **1**, the mesomorphism arose from the change in the binding mode of R from chelating to bridging during isotropization, while for **2**, the mesomorphisms arose from the breaking of the Cu-N_{bpy} bonds. The mesophases for **2** were cubic columnar (Cub, $P4_332$) and rectangular columnar (Col_R, space group *p2gg*) on cooling from 150 °C, Cub and hexagonal columnar (Col_H) on cooling from 184 °C (isotropic liquid phase), and Col_H and nematic columnar (Col_N) on cooling from 190 °C. These complexes were also photoluminescence upon charge transfer and *d-d* excitations. Finally, the Seebeck coefficient value (S_e) for **2** was -0.47 mV K^{-1}, identifying it as a potential thermoelectric material.

1. Introduction

A strategy that may be used in designing low dimensional magnetic, optical and electrical materials[1-3] is to combine the physical properties of liquid crystals (fluidity, molecular alignment, anisotropy, self-healing) into coordination polymers, forming polymeric metallomesogens.[4-6] An example is $[Cu_2(RCOO)_4(bpy)]_x$ (R = $(CH_3(CH_2)_7)_2CH$); bpy = 4,4'-bipyridine), which was mesomorphic at room temperature.[7] Its monomer was a copper(II) alkylcarboxylate, $[Cu_2(C_nH_{2n+1}COO)_4]$. These carboxylates are suitable monomers for the following reasons: (a) they are discotic mesogens ($n \geq 6$);[8,9] (b) most of them have known structures, known as dimeric paddle-wheel.[10-15] In this structure, bifunctional ligands (especially *N*-donors) may coordinate at the readily accessible axial positions to form polymers. In addition, the two magnetic and redox-active Cu(II) atoms are held in close proximity (Cu-Cu distance ~ 2.6 Å; $E_{Cu(II)/Cu(I)}$ ~ +0.5 – +0.8 V versus SCE[16]) by four bridging bidentate carboxylate ligands. This led to a strong antiferromagnetic coupling between the two copper(II) centres ($-J$ ~ 300 cm^{-1})[11,17] proposed to occur through the bridging carboxylate ligands, termed the super-exchange pathway,[11] and allowed them to act as multielectron redox catalysts; (c) they are easily prepared and thermally stable (decomposition temperatures > 200 °C);[7,14] and (d) alkylcarboxylate ions are relatively cheap and available in widely different structures (linear or branched chain, saturated or unsaturated).

We adopted the above strategy in our research for low-melting temperature mesomorphic coordination polymers. In our initial work, we chose $[Cu_2(R)_4(RH)_2]$ (R = 2-hexyldecanoate ion) as the monomer as it was a viscous green liquid at room temperature and exhibited a hexagonal columnar mesophase (Col_H) at – 23.2 °C.[14] However, we obtained two products from its reaction with bpy in ethanol when different work-up procedures were used: a violet crystalline solid, $[Cu(R)_2(bpy)_2].2RH$ (**1**), when the ethanolic reaction mixture was extracted with $CHCl_3$, and a green crystalline solid, $[Cu_2(R)_4(bpy)]_x$ (**2**), when C_2H_5OH was left to slowly evaporate at room temperature. In this paper, we report the structural, thermal, mesomorphic, and photoluminescent properties of **1** and **2**, and thermoelectric property for **2**. The structural formula for **1** was determined by single crystal X-ray crystallography, while the structural formula for **2** was proposed by comparing its analytical data with crystals of $[Cu_2(CH_3(CH_2)_5COO)_4(bpy)]_x$ (**3**) obtained from the reaction of $[Cu_2(CH_3(CH_2)_5COO)_4]$ with bpy under similar conditions (Scheme 1). Currently, we are unaware of any reports in the literature on similar effect of a solvent used in the work-up of a reaction mixture, although the influence of solvents in directing the structures of complexes formed during a reaction has been reported. For example, Zhu and Kitagawa obtained crystals of $\{trans\text{-}[Cu(Hsal)_2(bipy)](DMF)\}_x$ from the reaction of

Journal of Materials Chemistry C Accepted Manuscript

$[Cu_2(CH_3COO)_4(H_2O)_2]$, 2-$HOC_6H_4COOH$ (H_2sal) and bipy in a mixture of CH_3OH, DMF and H_2O, but obtained crystals of $[Cu_2(Hsal)_4(bipy)]_x$ from the same reaction in a mixture of H_2O and CH_3OH.[18]

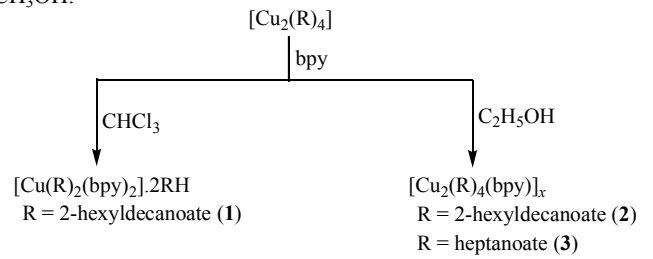

Scheme 1. The synthetic steps for **1** – **3**. The axial RH molecules are not shown in the structure of the reactant for complexes **1** and **2**.

2. Experimental section

2.1. Materials and general analytical instruments

The syntheses and characterisation of $[Cu_2(R)_4(RH)_2]$ (R = 2-hexyldecanoate ion) and $[Cu_2(CH_3(CH_2)_5COO)_4]$ were reported previously.[14] Other materials were commercially available and used as received. The elemental analyses for C, H and N were carried out on a Thermo Finnigan Flash EA 1112. The infrared spectra were obtained on a Perkin-Elmer Spectrum 400 spectrometer with samples as KBr pellets in the region 4000–400 cm^{-1}. The UV-vis spectra were obtained on a Shimadzu UV-vis-NIR 1600 spectrophotometer. The magnetic susceptibilities of solid samples were measured at room temperature with a Sherwood automagnetic susceptibility balance by the Gouy method, using $Hg[Co(NCS)_4]$ as the calibrant. The molar susceptibility values were corrected for the diamagnetism of the constituent atoms using Pascal's constants.

2.2. Syntheses

2.2.1. $[Cu(R)_2(bpy)_2].2RH$ (1). 4,4'-Bipyridine (0.12 g, 0.77 mmol) was added portion wise to a solution of $[Cu_2(R)_4(RH)_2]$ (0.87 g, 0.52 mmol) in hot C_2H_5OH (95%, 50 cm^3). The reaction mixture was then concentrated on a hot plate, allowed to cool, and the product extracted with $CHCl_3$. A violet crystalline solid deposited from the extract after a few days. Yield: 1.1 g (96.0%). CHN (%): Calc. C, 72.1; H, 10.2; N, 4.0. Found: C, 72.2; H, 10.7; N, 3.8. IR, cm^{-1}: 3049w, 2922s, 2852s, 1691m, 1602m, 1559s, 1462m, 1410s. The solid was recrystallised using $CHCl_3$ and C_2H_5OH (1:1 v/v), forming thin violet plates.

2.2.2. $[Cu_2(R)_4(bpy)]_x$ (2). 4,4'-Bipyridine (0.08 g, 0.54 mmol) was added portion wise to a solution of $[Cu_2(R)_4(RH)_2]$ (0.62 g, 0.37 mmol) in hot C_2H_5OH (95%, 50 cm^3). The reaction mixture was then concentrated on a hot plate and allowed to cool. A green crystalline solid deposited after a few days. Yield: 0.21 g (86.0%). CHN (%): Calc. C, 68.1; H, 10.2; N, 2.2. Found: C, 68.2; H, 10.7; N, 2.2. IR, cm^{-1}: 2921vs, 2853s, 1602vs, 1539w, 1455m, 1416s.

2.2.3. $[Cu_2(CH_3(CH_2)_5COO)_4(bpy)]_x$ (3). The method was the same as for **2**, using 4,4'-bipyridine (0.13 g, 0.82 mmol) and $[Cu_2(CH_3(CH_2)_5COO)_4]$ (0.52 g, 0.81 mmol). The product was green crystals. Yield: 0.42 g (65.0%). CHN (%): Calc. C, 57.1; H, 7.6; N, 3.5. Found: C, 56.8; H, 7.1; N, 3.7. IR, cm^{-1}: 2927vs, 2857s, 1608vs, 1419s.

2.3. X-ray crystallography

Single crystal X-ray diffraction data were collected on a Bruker SMART APEX II CCD fitted with Mo Kα radiation. The data set was corrected for absorption based on multiple scans[19] and reduced using standard methods.[20] The structure was solved by direct methods with SHELXS97[21] and refined by a full-matrix least-squares procedure on F^2 using SHELXL97 with anisotropic displacement parameters for non-hydrogen atoms and a weighting scheme of the form $w = 1/[\sigma^2(F_o^2) + aP^2 + bP]$, where $P = (F_o^2 + 2F_c^2)/3$). All hydrogen atoms were included in the final refinement in their calculated positions.

2.4. Thermal and mesomorphic studies

Thermogravimetry (TG) was performed on a Perkin-Elmer Pyris Diamond TG/DTA thermal instrument in the temperature range 50-900 °C under N_2 at a flow rate of 10 cm^3 min^{-1} and scan rate of 20 °C min^{-1}. Differential scanning calorimetry (DSC) was performed on a Mettler Toledo DSC 822 instrument under N_2 at a flow rate of 20 cm^3 min^{-1} and scan rate of 5 °C min^{-1}. The onset temperatures were quoted for all peaks observed. The optical textures were viewed under an Olympus polarising microscope equipped with a Mettler Toledo FP90 central processor and a Linkam THMS 600 hot stage. The heating and cooling rates were 5 and 2 °C min^{-1}, respectively, and the magnification was 50x. The small-and-wide angle X-ray scattering (SWAXS) patterns were recorded for **2** on an Anton Paar SAXSpace system employing a linear monochromatic Cu Kα beam (λ = 1.5405 Å). The powder was introduced into a TCS solid holder and heated at 150 °C for 30 min. The sample was then cooled using a Peltier temperature control, and the scattering data were collected from 140 °C to 50 °C. The measurement was then repeated by heating the powder in an oven at 184 °C for 15 min, cooled to 133 °C, and the data collected after it was kept at this temperature for 30 min. The total acquisition time was 4 h. Data processing was carried out using an Anton Paar SAXSquant software.

2.5. Photoluminescent study

The excitation and emission photoluminescence spectra were recorded for solutions of **1** and **2** in $CHCl_3$ on a PTI QuantaMaster™ 40 spectrofluorometer. The slit widths were set at a resolution of 10 nm for excitation and 5 nm for emission. The fluorescence lifetime was measured on a PTI TimeMaster (TM-200) LED-based Strobe Lifetime spectrofluorometer using the stroboscopic technique. The observed fluorescence decay was analyzed using PTI Felix GXTM data acquisition and analysis software. The data were recorded in 100 ps time intervals from 50 ns to 70 ns observation window. The instrument response function (IRF) was measured from the scattered light and estimated to be about 1.5 ns (full-width at half-maximum). The measured transients were fitted to multiexponential functions convoluted with the system response function. The fitting procedure was based on the Marquardt algorithm, where the experimental data were compared to a model decay convoluted with the IRF. The fit was judged by the value of the reduced χ^2.

2.6. Thermoelectric study

A solution, prepared by dissolving **2** (0.01 g) and KI-KI_3 (0.01 g) and/or tetrabutylammonium tetrafluoroborate (TBATFB; 0.3 g) in $CHCl_3$ (10 cm^3), was introduced into a two-compartment cell separated by a salt bridge containing the same solution. Each compartment contained a platinum wire electrode, which was cleaned using dilute HCl, followed by distilled water. The compartments were subjected to a temperature gradient by heating one cell and leaving the other at room temperature. The exact temperature of each solution was measured using a k-thermocouple,

Journal of Materials Chemistry C Accepted Manuscript

 This journal is © The Royal Society of Chemistry 2012

and the potential difference was measured by an Agilent 34461A Digital Multimeter. The potential difference between the hot side and the cold side was measured at about 2.5 °C intervals. Controlled experiments were done using solutions (similar molarities) of KI-KI_3 in $CHCl_3$ and in 3-methoxypropanonitrile (MPN), TBATFB in $CHCl_3$, and a mixture of TBATFB and KI-KI_3 in $CHCl_3$.

3. Results

3.1. Syntheses and structural studies

$[Cu(R)_2(bpy)_2].2RH$ (**1**), where R = 2-hexyldecanoate ion, was obtained as a violet solid from the reaction of $[Cu_2(R)_4(RH)_2]$ with 4,4'-bipyridine (bpy) when the reaction mixture was extracted with $CHCl_3$, while $[Cu_2(R)_4(bpy)]_x$ (**2**) was obtained as a green solid when the ethanolic reaction mixture was left to slowly evaporate at room temperature. Both solids were readily soluble in $CHCl_3$ and THF, partially soluble in DMSO, but insoluble in C_2H_5OH.

Complex **1** formed violet platelets using CH_3Cl-C_2H_5OH (1:1 v/v) as solvents. The X-ray data and structure refinement details for the single crystals are given in Table 1, and the selected bond lengths and angles are given in Table 2. The data indicate that the complex crystallized in the monoclinic *P21/n* space group. Its molecular structure (Fig. 1) shows two chelating bidentate 2-hexyldecanoato ligands at the basal plane and two bpy molecules at both axial positions of an elongated octahedral Cu(II) atom (CuO_4N_2 environment). The two Cu-O bond lengths were significantly different (1.969 Å and 2.468 Å) while the two Cu-N bond lengths were the same (2.009 Å). In addition, 2-hexyldecanoic acid molecules were H-bonded to the unbound N atom of each bpy molecule (O-H---N = 5.209 Å), and the two phenyl rings of bpy were at an angle of 21.6°. We noted that the molecular structure of **1** was similar to $[Cu(CH_3(CH_2)_8COO)_2(NH_3)_2].H_2O$[22] and $[Cu(4\text{-}HO_6H_4COO)_2(pyr)_2]$.[23]

(a)

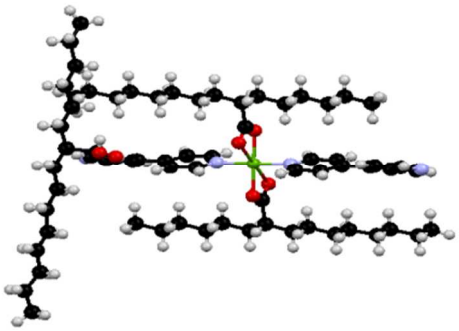

(b)

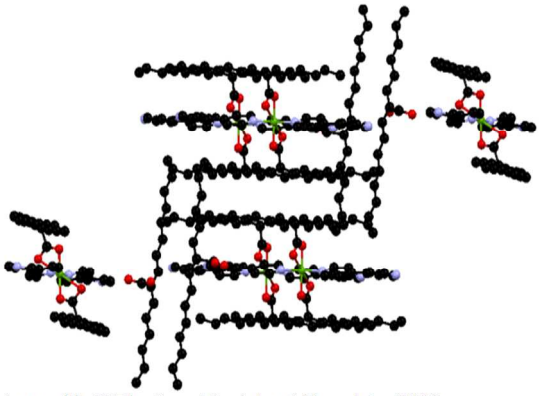

Fig. 1 (a) Molecular structure of **1**; and (b) its packing pattern (H atoms were omitted for clarity), viewed along the *b* axis.

Table 1 Crystallographic data for **1** and **3**

Complex	**1**	**3**
Empirical formula	$C_{84}H_{142}CuN_4O_8$	$C_{19}H_{30}CuNO_4$
Formula weight	1399.57	399.98
Crystal system	Monoclinic	Monoclinic
Space group	*P21/n*	*C2/c*
T (K)	293(2)	100(2)
a (Å)	11.8993(8)	16.873(3)
b (Å)	8.4256(3)	25.268(5)
c (Å)	42.389(2)	10.680(2)
α (°)	90	90
β (°)	93.892(5)	119.457(2)
γ (°)	90	90
Z	2	8
V (Å^3)	4240.1(4)	3964.6(14)
ρ(calcd) (g cm^{-3})	1.096	1.340
μ (mm^{-1})	0.310	1.123
F(000)	1534	1696
θ range (°)	2.89 – 26.00	1.60 - 27.50
Max/min transmission	-	0.6684, 0.5927
Index ranges	$-14 \le h \le 14$	$-20 \le h \le 21$
	$-10 \le k \le 10$	$-32 \le k \le 32$
	$-52 \le l \le 41$	$13 \le l \le 8$
Reflections collected	26693	13086
Independent reflections, R_{int}	8336, 0.0751	4527, 0.0637
Completeness to θ	99.9 %	99.5 %
	8325/66/443	4527/0/228
Goodness-of-fit on F^2	1.133	1.000
Final *R* indices [$I > 2\sigma$(I)]	$R_1 = 0.1580$	$R_1 = 0.0450$
	$wR_2 = 0.3500$	$wR_2 = 0.1049$
R indices (all data)	$R_1 = 0.1905$	$R_1 = 0.0778$
	$wR_2 = 0.3718$	$wR_2 = 0.1207$
$\Delta\rho_{max}$, $\Delta\rho_{min}$ (e Å^{-3})	0.802, -0.541	0.529, –0.838

Table 2. Selected bond lengths (Å) and angles (°) for **1** and **3**

Complex	**1**	**3**
Bond length		
Cu-Cu	-	2.6147
Cu-O	1.969, 2.468	1.973
Cu-N	2.009	2.146
Angle		
O(1)-Cu-O(2)	57.92, 122.08	88.16, 91.96
N-Cu-O	89.34	95.83, 97.35
N(1)-Cu-N(2)	180.0	-

We also recorded other instrumental data for **1** (Table 3). The CHN analyses (Experimental) were in excellent agreement with the molecular formula deduced from the X-ray data. Its FTIR spectrum showed peaks at 1602 cm^{-1}, 1462 cm^{-1}, 1375 cm^{-1}, and 1217 cm^{-1} for coordinated bpy,[24] two strong peaks at 2922 cm^{-1} and 2852 cm^{-1} for $\upsilon_{asym}CH_2$ and $\upsilon_{sym}CH_2$, respectively, a medium peak at 1691 cm^{-1} for C=O of H-bonded RH, and two strong peaks at 1559 cm^{-1} and 1410 cm^{-1} for $\upsilon_{asym}COO$ and $\upsilon_{sym}COO$, respectively. Accordingly, the Δ value ($\Delta = \upsilon_{asym}COO - \upsilon_{sym}COO$ = 149 cm^{-1}) was in agreement with the chelating bidentate binding mode of the carboxylato ligand.[24,25] Its electronic absorption spectrum in $CHCl_3$ showed two *d-d* bands at 700 nm (ε_{max} = 218 M^{-1} cm^{-1}) and 383 nm (ε_{max} = 127 M^{-1} cm^{-1}). The band at 700 nm was broad and arose from the electronic transitions from $^2B_{1g}$ to E_{1g}, $^2B_{2g}$ and $^2A_{1g}$ of a distorted octahedral Cu(II) atom.[26] Finally, its effective magnetic moment (μ_{eff}), calculated from the equation: $\mu_{eff} = 2.83[T(\chi_M^{corr} - N\alpha)]^{½}$, where χ_M^{corr} = corrected molar magnetic susceptibility, *T* = absolute temperature, and $N\alpha$ = temperature-independent paramagnetism (60

Journal of Materials Chemistry C Accepted Manuscript

x 10^{-6} cm^3 mol^{-1} per Cu(II)), was 1.85 BM at 298 K. The value was in agreement with literature data for magnetically dilute Cu(II) octahedral complexes (1.9-2.2 BM).[27]

Table 3 Spectroscopic and magnetic data for **1 - 3**

Complex	Δ* (cm^{-1})	λ_{max}/nm (ε_{max}/M^{-1} cm^{-1})	μ_{eff} (BM)
$[Cu(R)_2(bpy)_2].2RH$ (**1**)	149	700 (218), 383 (127)	1.85
$[Cu_2(R)_4(bpy)]_n$ (**2**)	186	700 (387), 400 (209)	1.59
$[Cu_2(R')_4(bpy)]_n$ (**3**)	192	683 (500), 380 (314)	1.67

*Δ = υ_{asym}COO – υ_{sym}COO from IR spectroscopy; R = 2-hexyldecanoate ion; R' = heptanoate ion

(a)

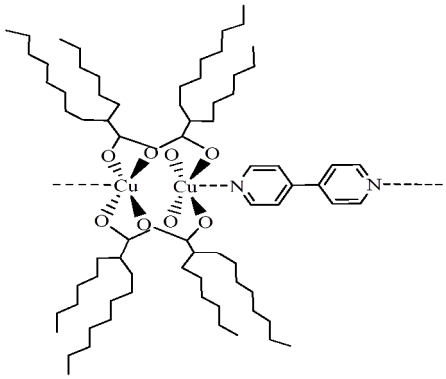

(b)

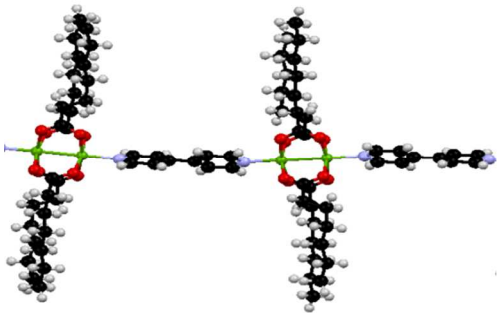

(c)

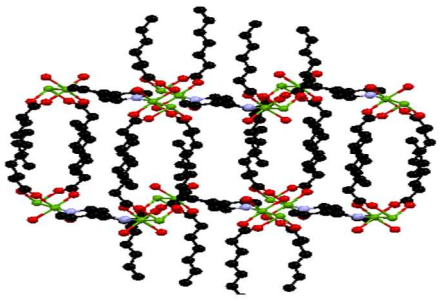

Fig. 2 (a) Proposed structure for **2**, (b) Molecular structure for **3**, showing two repeat units, and (c) packing diagram for **3** viewed along the *b* axis (hydrogen atoms were removed for clarity

In contrast, **2** did not form good quality single crystals. Hence, its structural formula (Fig. 2a) was deduced from combined instrumental data and by comparison with data for crystals of $[Cu_2(CH_3(CH_2)_5COO)_4(bpy)]_x$ (**3**). These are shown in Table 3. Firstly, the CHN elemental analyses (Experimental) for **2** were in excellent agreement with the formula for the repeat unit, $[Cu_2(RCOO)_4(bpy)]$. Its FTIR spectrum showed peaks for CH_2 and bpy at almost the same wavenumbers as for **1**, and two strong peaks at 1602 cm^{-1} and 1416 cm^{-1} for υ_{asym}COO and υ_{sym}COO, respectively. Accordingly, the Δ value was 186 cm^{-1}, suggesting bridging bidentate 2-hexyldecanoato ligand.[24,25] Its electronic absorption spectrum, recorded in $CHCl_3$, shows two broad *d-d* bands at 700 nm (ε_{max} = 387 M^{-1} cm^{-1}) and 400 nm (ε_{max} = 209 M^{-1} cm^{-1}), suggesting a square pyramidal geometry[28] at both Cu(II) centres. Its μ_{eff} value, calculated for the dimeric repeat unit, was 1.59 BM at 298 K. The value was comparable with **3** (1.67 BM), but significantly lower than $[Cu_2(2,2\text{-(dioctyl)acetato})_4(bpy)]_x$ (1.8 BM).[7]

Complex **3** crystallised in the monoclinic space group *C2/c* (Table 1). Its molecular structure (Fig. 2b), shows the paddle-wheel dimers linked by bpy molecules at the axial positions to form a linear-chain polymer. The dimeric unit showed a pair of chains opposite one another in an all-*trans* configuration, while the other two chains contained one gauche link. All of the Cu–O bond lengths (1.973 Å) and Cu–N bond lengths (2.146 Å) were the same, while the Cu-Cu separation was 2.6147 Å (Table 2), the distance between two paddle-wheel dimers was 11.359 Å, and the dihedral angle (α) between two phenyl ring of bpy was 33.1°.

Studies on linear chain coordination polymers involving bpy as a linker have established a correlation between the magnetic interaction between the metal centres and α, as follows: the interaction is strongly antiferromagnetic when α = 0°, and strongly ferromagnetic when α = 90°. The parameter for the magnetic interaction is 2*J*, which has a negative value if antiferromagnetic and a positive value if ferromagnetic. For example, α = 7.5° and 2*J* = -177 cm^{-1} for $[Cu_2(2,2'\text{-bpy})_2(4,4'\text{-bpy})(L)_2](ClO_4)_2.H_2O]_x$ (L = 4-$H_2NC_6H_4COO$).[29] For **3**, the value for α was 33.1°, hence its 2*J* value was expected to be less negative than -177 cm^{-1} (weaker antiferromagnetic coupling). Since the μ_{eff} value for **2** (1.59 BM) was lower (stronger antiferromagnetic coupling) than **3** (μ_{eff} = 1.67 BM), it may be inferred that for **2**, the 2*J* value was more negative than **3** and the dihedral angle of bpy in this complex was 33.1° > α > 7.5°.

3.2. Thermal and mesomorphic studies

Prior to studying the mesomorphic properties of **1** and **2**, we determined their decomposition temperatures by thermogravimetry (TG). The TG trace showed that **1** suffered a major weight loss of 89.5% (calc. 95.5%) at 240 °C, while **2** suffered a major weight loss of 90.7% (calc. 90.3%) at 220 °C. The similar thermal stabilities for these complexes were not surprising since their decomposition was initiated by the decarboxylation[30] of 2-hexyldecanoato ligand.

The mesomorphic properties of these complexes were initially studied by DSC and POM. The DSC traces (Fig. 3) and data (Table 4) were recorded on both heating and cooling modes. For **1**, the traces were recorded in the temperature range 30 – 170 °C. There was a strong endothermic peak at 52.3 °C (ΔH = +113.1 kJ mol^{-1}) and a weak exothermic peak at 81.0 °C (ΔH ~ -5 kJ mol^{-1}) on heating, and an exothermic peak at 66.3 °C (ΔH = -29.7 kJ mol^{-1}) on cooling. When viewed under POM, the sample was observed to be a fluid at 44 °C and to clear to the isotropic liquid phase (I) at about 70 °C. However on further heating, elongated optical textures were observed at 76.7 °C (Fig. 4a), which then cleared at 78 °C. On cooling from 98.5 °C, an optical texture formed at 73.6 °C (Fig. 4b). This texture continued to grow on further cooling to 30 °C but the sample remained fluid at this temperature. On reheating, the texture cleared at 81 °C, and on cooling reappeared at 71.9 °C (Fig. 4c). Combining both the DSC and POM results, we proposed that on

Journal of Materials Chemistry C Accepted Manuscript

This journal is © The Royal Society of Chemistry 2012

initial heating, the two RH molecules, which was hydrogen-bonded to the unbound N atom of bpy at the axial positions, dissociated from the complex. The freed RH molecules (melting point = 18 °C) explained the observed fluidity at 44 °C. On further heating, the binding mode of R in $[Cu(R)_2(bpy)_2]$ (Cr1) changed from chelating to bridging as evidenced from the weak exothermic peak at 81 °C, leading to the formation of a polymeric complex, $[Cu(R)_2(bpy)_2]_n$ (Cr2). Similar change in the binding mode of carboxylato ligands on heating was suggested by Moita *et al.* for $[Cu_2(CH_3(CH_2)_nCOO)_4]$ (n = 4 – 8, 10, 12, 14, 16) based on variable-temperature FTIR spectroscopy.[31]

The DSC traces for **2** were recorded in the temperature range of 30 – 190 °C. On heating, there was a strong endothermic peak at 48.3 °C (ΔH = +35.7 kJ mol^{-1}) and two weak endothermic peaks at 131.7 °C and 151.7 °C, and on cooling, three corresponding exothermic peaks with similar enthalpies. Viewed under POM, the sample started to clear at 184 °C, and on cooling from this temperature, dendritic optical textures of a Col_H mesophase[32-34] was observed at 180.6 °C (Fig. 4d). This mesophase coalesced on further cooling to a mosaic texture with homeotropic region at 133 °C (Fig. 4e), that persisted on further cooling to 30 °C. When a new sample was heated to 190 °C (above its isotropization temperature), the dendritic textures reappeared on cooling at almost the same temperature as before, followed by nematic globules (Col_N)[32-34] at 160 °C (Fig. 4f).

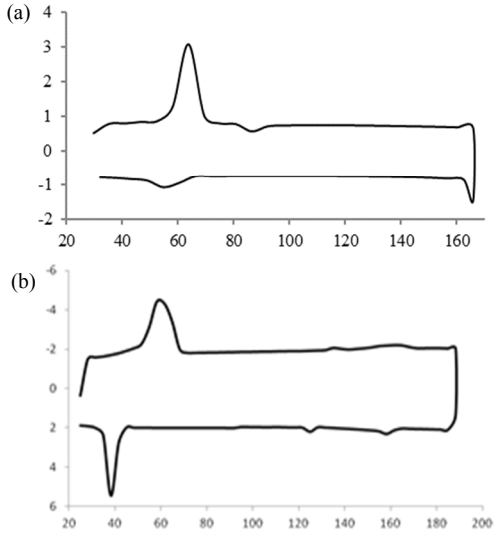

Fig. 3 DSC traces for **1** (a) and **2** (b). Heating (top scan), cooling (bottom scan), endothermic peak (up).

Table 4. DSC data for **1** (30 – 170 °C) and **2** (30 – 190 °C)

Complex	Mode	T_{onset} (°C)	ΔH (kJ mol^{-1})	Phase transition
1	heating	52.3	+113.1	Cr1 – I
		81.0	~ -5	I – Cr2
	cooling	66.3	-29.7	Cr2 – M
2	heating	48.3	+35.7	Cr – (Cub, Col_R)
		131.7	~ +1	(Cub, Col_R) – Col_H
		151.7	~ +1	Col_H – I
	cooling	161.7	~ -1	I – (Col_H, Col_N)
		128.3	~ -1	Col_H – Cub
		45.0	-34.9	Cub – Cr

Cr = crystal; I = isotropic liquid; M = mesophase; Col_H = hexagonal columnar; Cub = cubic columnar; Col_R = rectangular columnar; Col_N = nematic columnar

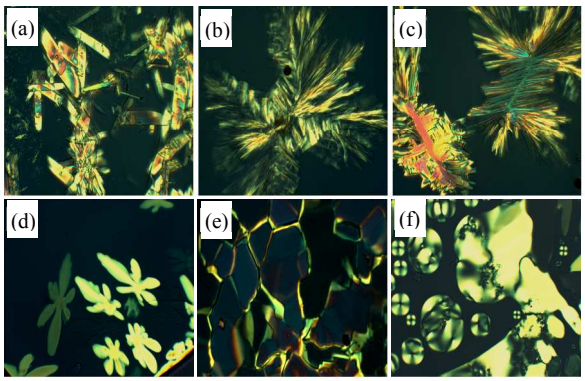

Fig. 4 Photomicrographs of (a) **1** at 76.7 °C on heating, (b) **1** at 73.6 °C on cooling from 98.5 °C, (c) **1** at 71.9 °C on cooling from 81.0 °C, (d) **2** at 180.6 °C on cooling from 185 °C, (e) **2** at 133 °C on cooling from 185 °C, and (f) **2** at 160 °C on cooling from 190 °C.

The mesomorphisms exhibited by **2** were then ascertained by SWAXS experiments. Initially, the sample was heated at 150 °C for 30 min (below its clearing temperature) to ensure that the Cu-N_{bpy} bonds were not broken (reported to occur at about 170 °C[7]). The X-ray data were then recorded on cooling from 140 °C to 50 °C (Fig. 5a).

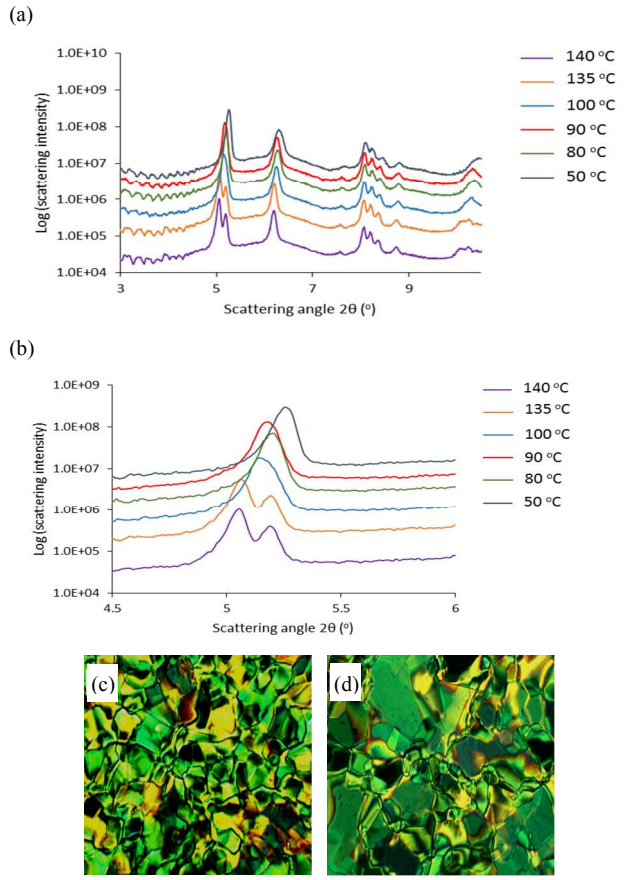

Fig. 5 XRD patterns of **2** (a) at different temperatures on cooling from 150 °C, (b) the two most intense peaks, and its photomicrographs captured after 30 min (c) on heating at 150 °C, and (d) on cooling to 100 °C.

From the most intense peak at each temperature, the lattice spacing (d) and domain size (D) were calculated using the Bragg

Journal of Materials Chemistry C Accepted Manuscript

equation ($n\lambda = 2d \sin\theta$) and Scherrer expression ($D = 0.99\ \lambda/(\beta_{½} \cos\theta$, where $\lambda = 1.5405$ Å, $n = 1$, and $\beta_{½}$ = full-width at half-maximum (FWHM) of the Bragg peak), respectively (Table 5). The results show that the d values decreased from 17.45 Å at 140 °C to 16.82 Å at 50 °C, while the domain size decreased from 1232 Å at 140 °C to a minimum value of 791 Å at 100 °C and then increased to 1031 Å at 50 °C. Using the X-ray crystallographic data for **3** as a model for the molecular structure of the rigid core in **2** (their geometry and macroscopic organization are poorly affected by the melting process), the measured length (l) of repeat unit ([$Cu_2(R)_4$(bpy)]) was 13.96 Å. Accordingly, we infer that **2** was made up of about 88 repeat units at 140 °C, 57 at 100 °C and 74 at 50 °C.

We observed that the two intense peaks at 140 °C and 135 °C (2θ = 5.06° and 5.14°, respectively) merged at 100 °C, and then shifted slightly towards larger 2θ values on further cooling down to 50 °C (Fig. 5b). These observations signalled a transition from a phase of lower symmetry and larger dimension (hexagonal columnar) to that of higher symmetry and smaller dimension (rectangular columnar). With the exception for the patterns at 140 °C and 50 °C, the other peaks may be indexed to a mixture of mainly rectangular columnar mesophase (Col_R; space group *p2gg*; lattice parameters: $a = 28.2$ Å, $b = 21.6$ Å) and cubic columnar mesophase (Cub; space group $p4_332$; lattice parameter: $a = 24.2$ Å), as shown for T = 100 °C in Fig. 6 and Table 6. From these parameters, the number of repeat units (Z) per unit cell may be calculated using the equation: $Z = (\rho.N_A.V.10^{-24})/FW$, where ρ = density of the mesophase (assumed ~ 1 g cm^{-3}), N_A = Avogadro's number, V = volume of the unit cell, and FW = formula weight of the repeat unit (1304.94 g mol^{-1}). For the Col_R mesophase, $S = 609$ Å^2, $h = 13.96$ Å, $V = Sh = 8502$ Å^3, $Z = 4$. Similarly for the Cub mesophase, Z = 6.5 ~ 7. We noted that [Cu_2(2,2-dioctylacetato)$_4$(pyrazine)]$_x$, a coordination polymer similar to **2**, was mesomorphic at 95 °C, but the authors could not index the reflections to any specific lattice.[7]

Table 5 Lattice spacing (d), domain size (D) and number of repeat units (ru) for **2** at different temperatures on cooling from 150 °C

T (°C)	2θ (°)	d (Å)	D (Å)	ru
140	5.06	17.45	1232	88
135	5.14	17.18	1171	84
100	5.15	17.14	791	57
90	5.18	17.05	916	66
80	5.19	17.01	1012	72
50	5.25	16.82	1031	74

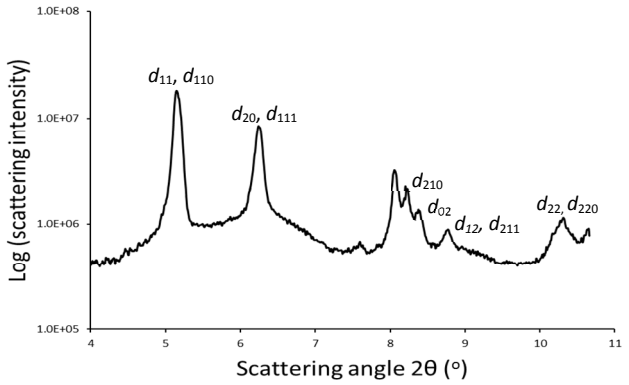

Fig. 6 The XRD pattern for **2** at 100 °C on cooling from 150 °C.

Table 6 XRD data for **2** at 100 °C on cooling from 150 °C

2θ (°)	d (Å)	ratio	hk (Col_R)	hkl (Cub)	Lattice parameters
5.15vs	17.14	1	11	110	Col_R (*p2gg*):
6.26s	14.11	1.21	20	111	$a = 28.2$ Å
8.08m	10.93	1.57	?	?	$b = 21.6$ Å
8.23w	10.73	1.60	-	210	$S = 609$ Å^2
8.40vw	10.52	1.63	02	-	Cub ($p4_332$):
8.79vw	10.05	1.71	12	211	$a = 24.2$ Å
10.32vw	8.56	2.01	22	220	$V = 14172$ Å^3

The reflection intensities of the peaks are denoted as very strong (vs), strong (s), medium (m), weak (w), and very weak (vw). hk and hkl = lattice planes, d = observed lattice spacing, a and b = lattice parameters (Col_R: $1/d_{hk} = (h^2/a^2 + k^2/b^2)^{½}$; Cub: $d_{hkl} = a/(h^2 + k^2 + l^2)^{½}$), S = lattice area, and V = volume of unit cell.

The SWAXS experiment was then repeated for **2** to ascertain the mesophase at 133 °C (Fig. 4e), observed on POM to form from the Col_H mesophase on cooling from 185 °C. The XRD pattern, taken after the sample was heated to 184 °C (isotropic liquid phase), is shown in Fig. 7, and the corresponding parameters are shown in Table 7. It reveals seven sharp reflections at small 2θ values (3° < 2θ < 16°) which permit an unambiguous assignment of a cubic lattice (Cub) with lattice parameter $a = 24.5$ Å. A broad halo centred at around 4.6 Å indicates molten alkyl chains typical of a liquid crystalline state. The lattice is non-centred, and belongs to the $p4_332$ space group, as shown by the presence of reflection 7, (410), ($h + k$ = 2n + 1). The domain size (D) was 351.2 Å, which translates to about 25 repeat units. This was significantly lower than 84 repeat units at about the same temperature (135 °C) when the sample was cooled from 150 °C (Table 5).

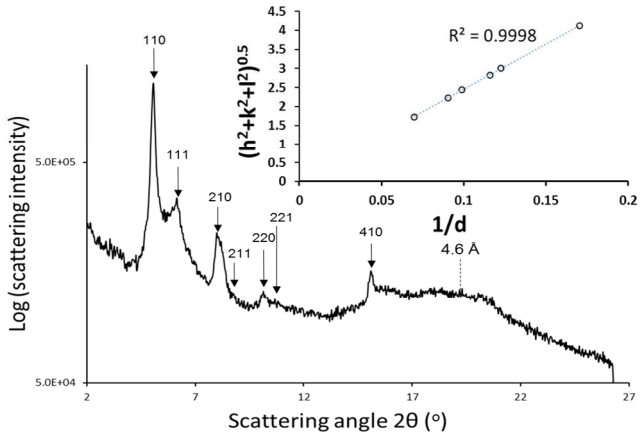

Fig. 7 The XRD pattern for **2** at 133 °C on cooling from 184 °C.

Table 7. Detailed indexing of **2** at 133 °C

Peak	hkl	d_{obs} (Å)	d_{calc} (Å)	Lattice parameters
1 vs	110	17.34	17.32	Cub ($p4_332$)
2 m	111	14.28	14.15	$a = 24.5$ Å
3 m	210	11.05	10.96	V = 14706 Å^3
4 vw	211	10.10	10.00	
5 w	220	8.67	8.66	
6 vw	221	8.16	8.17	
7 w	410	5.86	5.94	

The reflection intensities of the peaks are denoted as very strong (vs), medium (m), weak (w), and very weak (vw). hkl = lattice planes, d_{obs} = observed lattice spacing, and d_{calc} = calculated lattice spacing ($d_{calc} = a/(h^2 + k^2 + l^2)^{½}$).

Journal of Materials Chemistry C Accepted Manuscript

This journal is © The Royal Society of Chemistry 2012

Based on the above findings, we propose that the different mesomorphisms exhibited by **2** at different temperatures arose mainly from the effect of heat on the chain length of the polymer, while the Cu-R bonds were not cleaved. The latter argument was based on the deduction from EXAFS study on copper(II) carboxylates that the oligomeric chains remained intact in the molten state.[35] Hence on heating, the Cu–N_{bpy} bonds of the polymer were broken at about 170 °C,[7] resulting in shorter oligomers. Accordingly, the Col_R and Cub mesophases arose from the oscillation of the columns formed by the different length oligomers, while the Col_N mesophase arose from shorter chain oligomers due to a more extensive breaking of Cu–N_{bpy} bonds at temperatures above its isotropic liquid phase."

Molecular models for the Col_H and Col_R mesophases, proposed by Rusjan *et al*. for rhodium(II) carboxylate coordination polymers,[36] may apply for **2** as they have similar structure. Also, a model specifically for the Col_R mesophase (plane group *p2gg*) was proposed for a cobalt(II) complex.[37] These models may apply for the Col_R mesophase for **2** as it belongs to the same plane group. Suggested structures for both phases are shown in Fig. 8.

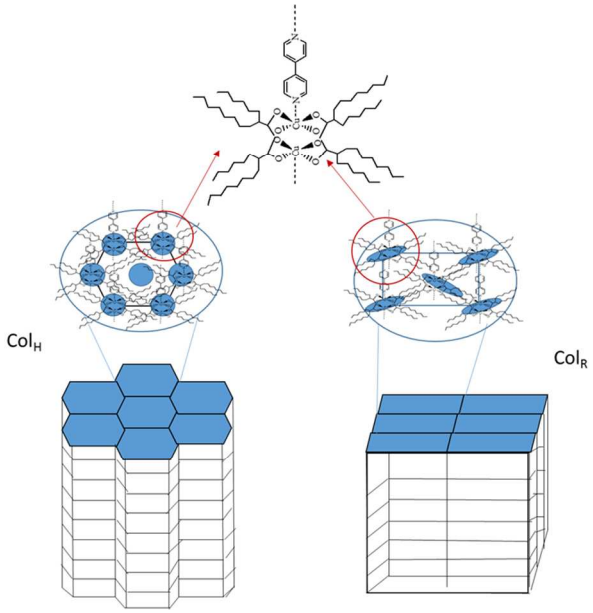

Fig. 8 Proposed molecular models for the Col_H and Col_R phases of **2**.

3.3. Photoluminescent and thermoelectric studies

Coordination polymers with luminescent and charge-transport properties represent a new class of multifunctional materials. Hence, we proceeded to study the photoluminescent and thermoelectric properties of **2**, and for comparison, the photoluminescent properties of **1**.

Table 8 Photoluminescent data for **1** and **2**

λ_{ex} (nm)	Complex **1**			Complex **2**		
	λ_{em} (nm)	Δ (nm)	τ (ns)	λ_{em} (nm)	Δ (nm)	τ (ns)
302	332	30	0.89	350	48	1.97
390	394	4	0.37	416	22	0.65
700	706	6	0.19	714	14	0.42

Δ = Stokes shift, λ_{ex} = excitation wavelength, λ_{em} = emission wavelength

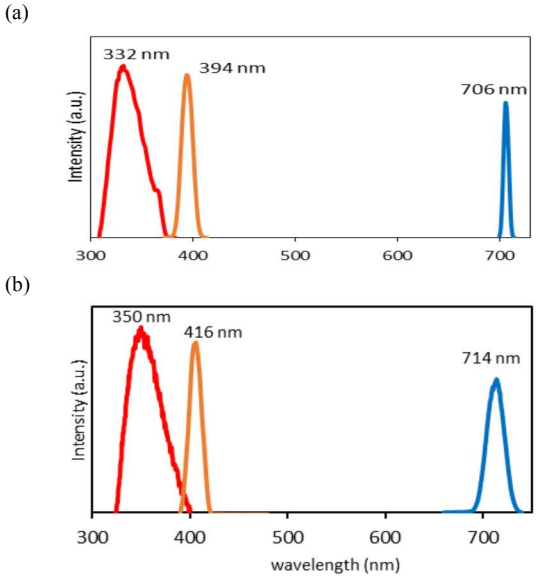

Fig. 9 Photoluminescent spectra of (a) **1** and (b) **2** upon excitations at 302 nm (red), 390 nm (brown) and 700 nm (blue).

The photoluminescence spectra for **1** and **2** (Fig. 9) and the corresponding data (Table 8) indicate that both complexes were luminescence upon excitations at 302 nm, which corresponds to the ligand-to-metal charge transfer transition (LMCT), and at 390 nm and 700 nm, which correspond to the *d-d* transitions. Under these conditions, **2** has wider Stokes shifts (14 – 48 nm) and longer lifetimes of the excited complex (τ = 0.42 – 1.97 ns) compared to **1** (Stoke shifts = 6 – 30 nm; τ = 0.19 – 0.89 ns). These results are expected and may be attributed to the longer conjugation length of the polymeric complex. Also, both complexes have better luminescent properties arising from the intraligand π*-π transition upon LMCT excitation. Luminescence arising from LMCT excitation has been observed for a few Cu(II) complexes. For example, a solution of $[Cu_2(1,10\text{-phen})_2(H_2O)_4(cbtc)].6H_2O$ (phen = phenanthroline, cbtc = 1,2,3,4-cyclobutanetetracarboxylate tetraanion) in CH_3OH-$CHCl_3$ showed luminescence at 358 nm upon excitation at 262 nm,[38] while two 1-D coordination polymers, $[CuL_2(NSC)_2]_x$ and $[CuL_2(NO_3)_2]_x$ (L = $(C_5H_4N)C(CH_3)$=N-N=$C(CH_3)(C_5H_4N)$), showed luminescence at 337 nm and 316 nm, respectively, upon excitation at 220 nm in the solid state.[39] These complexes were excited at higher energies, and hence have larger Stokes shifts (96 nm and 117 nm) when compared to **1** and **2**. However, we are unaware of any Cu(II) complexes showing luminescence upon the *d-d* excitations.

In addition, the lifetimes for the excited complexes of **1** and **2** were very short compared to other complexes reported in the literature, such as $[Ru(bpy)_2(dppz)]^{2+}$ (τ = 185 ns)[40] and Ir(2-phenylpyridine)$_2$(sol)$_2$ (τ = 487 ns).[41] This is because for copper(II) complexes, their ligand field states were at a lower energy than the antibonding π* orbital(s) of 4,4'-bpy ligand. Hence, upon ligand-to-metal charge-transfer transition (LMCT), the low-lying ligand field states effectively deactivated the initially populated CT state.

Journal of Materials Chemistry C Accepted Manuscript

However, the lifetimes of these complexes were sufficiently long to allow for the electron(s) to be ejected into the conduction band of TiO_2 in dye-sensitised solar cells, reported to occur within femtoseconds.[42] Accordingly these complexes are attractive alternatives as photoactive materials as they were easy to prepare using readily available and cheap starting materials, nontoxic and heat- and air-stable.

Furthermore, the width of the lowest energy peak for **1** was narrower than that of **2**, while those of higher energy peaks for both complexes were similar. The width of a peak is proportional to the degree of geometrical distortion upon electronic transition. For the *d-d* transition, the excited electron occupied the antibonding $d_{x^2-y^2}$ orbital of copper(II) atom, hence weakening the Cu-R bonds. Since **1** (a mononuclear complex) has a more rigid structure than **2** (a linear-chain coordination polymer), the former experienced less geometrical distortion. This effect was more pronounced for the lowest energy transitions as the relaxation times for both excited complexes were very short (τ = 0.19 ns for **1** and 0.42 ns for **2**).

Thermoelectricity involves the conversion of thermal energy directly to electrical energy. An important parameter for evaluation of the thermoelectric performance for a solution is the Seebeck coefficient (S_e), which is defined by the voltage generated per Kelvin. The value of S_e can be determined from the slope of a linear graph of ΔV versus ΔT, where ΔV is the potential difference for a given temperature interval, ΔT. The factors that determine the magnitude and sign of S_e are the entropy change and charge of the carrier, respectively. As examples, the value of S_e was +1.4 mV K^{-1} for $[Fe(CN)_6]^{3-/4-}$,[43] +2.19 mV K^{-1} for $[Co(bipy)_3]^{2+/3+}[Tf_2N]_{2/3}$,[44] and +1.89 mV K^{-1} for $[Co(L)_2]^{2+/3+}(BF_4)_{2/3}$.[37] The good thermoelectric properties of these mixed-valence SCO complexes were ascribed to increased entropies of their cations (positive S_e values).

For **2**, we performed preliminary experiments to determine its S_e values in $CHCl_3$ in the presence of a redox couple, KI-KI_3 (standard potential = +0.35 V versus NHE) and/or an electrolyte, tetrabutylammonium tetrafluoroborate (TBATFB). As comparisons, we also determined the S_e values for KI-KI_3 and a mixture of KI-KI_3 and TBATFB in the same solvent. The results are shown in Fig. 10 and Table 9. To check the reliability of our experimental procedure, the S_e value of KI-KI_3 in 3-methoxypropanonitrile (MPN) was also determined. The result (+0.36 mV K^{-1}) was similar to that reported in the literature (+0.34 mV K^{-1}).[45]

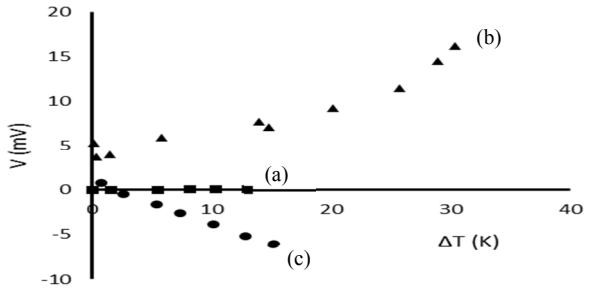

Fig. 10 Graphs of ΔV versus ΔT for solutions of **2** in $CHCl_3$ in the presence of (a) KI-KI_3, (b) TBATFB and (c) KI-KI_3 and TBATFB.

Table 9 S_e values of several solutions in $CHCl_3$

Solution	S_e (mV K^{-1})
KI-KI_3	-0.025
KI-KI_3 and TBATFB	+0.57
2 and KI-KI_3	+0.005
2 and TBATFB	+0.35
2, KI-KI_3 and TBATFB	-0.47

It is interesting to note that the thermoelectric properties of **2** (magnitude and sign of S_e) depended on the presence of KI-KI_3 and TBATFB. The polymeric structure of **2** was expected to be retained in solution, as suggested for similar complexes.[46,47] KI-KI_3 is a redox couple, and may react with **2** in two ways: (a) two-electron oxidation by I_3^- ion to form $[Cu^{III}Cu^{III}(R)_4(bpy)]_x^{2+}$ cation (Equation 1), and/or (b) one-electron reduction by I^- ion to form $[Cu^{II}Cu^{I}(R)_4(bpy)]_x^-$ anion (Equation 2).[48] The formation of the anion is expected to be more facile since Cu(II) is more readily reduced than oxidised.

Equation 1 (two-electron oxidation):
$[Cu^{II}Cu^{II}(R)_4(bpy)]_x + I_3^- \longrightarrow [Cu^{III}Cu^{III}(R)_4(bpy)]_x^{2+} + 3I^-$

Equation 2 (one-electron reduction):
$[Cu^{II}Cu^{II}(R)_4(bpy)]_x + 2I^- \longrightarrow [Cu^{II}Cu^{I}(R)_4(bpy)]_x^- + I_2^-$

The S_e value of **2** in the presence of KI-KI_3 was very low (+0.005 mV K^{-1}), indicating the inability of the ions present to act as charge carriers. In contrast, the S_e value in the presence of TBATFB was +0.35 mV K^{-1} (however, the graph was not linear). We ascribe the positive value to $(CH_3CH_2CH_2CH_2)_4N^+$ ion of TBATFB as the dominant charge carrier since it has a higher mobility (more lyophilic) than BF_4^- ion in $CHCl_3$. Surprisingly, the S_e value in the presence of both KI-KI_3 and TBATFB were -0.47 mV K^{-1}. The negative value suggests that the mixed-valence formed, $[Cu^{II}Cu^{I}(R)_4(bpy)]_x^-$ (Equation 2), dissociated to $[Cu^{II}Cu^{I}(R)_3(bpy)]_x$ and R^- ion (the dominant charge carrier). These results suggest that **2** is a promising thermoelectrical material. We are currently optimising its thermoelectric properties with respect to other parameters, such as concentration and solvent polarity.

4. Conclusion

$[Cu(R)_2(bpy)_2].2RH$ (**1**) was a mononuclear molecule while $[Cu_2(R)_4(bpy)]_x$ (**2**) was a linear-chain dinuclear coordination polymer. Both complexes were thermally stable, have low melting temperatures (about 50 °C), and exhibited temperature-dependent mesomorphisms. The mesomorphism observed for **1** arose from the change in the binding mode of 2-hexyldecanoato ligand from chelating to bridging during isotropization. The mesophases for **2** were cubic columnar and rectangular columnar on cooling below its isotropic liquid phase (I), hexagonal columnar and cubic columnar on cooling from I, and hexagonal columnar, nematic columnar, and cubic columnar on cooling from temperatures higher than I. The different mesophases exhibited by **2** arose from the breaking of Cu-N_{bpy} bonds at temperatures above 170 °C. Complexes **1** and **2** were also photoluminescence in solution upon both metal-to-ligand charge transfer and *d-d* excitations. As expected, **2** has better photoluminescent properties in terms of wider Stokes shifts and longer lifetimes of the excited complex than **1**. Thermoelectric study was done for **2** only. Its Seebeck coefficient value (S_e) in the presence of a mixture of KI-KI_3 and TBATFB was -0.47 mV K^{-1}, and was initiated by the one-electron reduction of $[Cu^{II}Cu^{II}(R)_4(bpy)]_x$ to $[Cu^{II}Cu^{I}(R)_4(bpy)]_x^-$ by I^- ion, followed by dissociation of R^- from the mixed-valence anionic polymer. Accordingly, **2** is an example of a multifunctional low-melting temperature metallomesogenic linear-chain coordination polymer.

Acknowledgements

The authors thank Malaysia Ministry of Education for High Impact Research Grants (UM.C/625/1/HIR/MOHE/05 and UM.C/625/1/HIR/MOHE/ENG/29), and University of Malaya for research grants (RP014A-13AET, PG023-2013A and PV056-

Journal of Materials Chemistry C Accepted Manuscript

 This journal is © The Royal Society of Chemistry 2012

2012A). We are also grateful to Prof. D. W. Bruce from the Chemistry Department, York University, York, UK for the discussion on mesophases, and Dr. Arief C. Wibowo from the Chemistry Department, Science Faculty, University of Malaya for the discussion on PL and XRD data.

Notes and references

[a] Chemistry Department, Science Faculty, Universiti Malaya, 50603 Kuala Lumpur, Malaysia.

[b] Electrical Engineering Department, Engineering Faculty, Universiti Malaya, 50603 Kuala Lumpur, Malaysia.

† CCDC-1056411 (for **1**) and 909604 (for **3**) contain the supplementary crystallographic data. These data can be obtained free of charge *via* http://www.ccdc.cam.ac.uk/conts/retrieving.html, or from the Cambridge Crystallographic Data Centre, 12 Union Road, Cambridge CB2 1EZ, UK; fax: (+44) 1223 336033; or e-mail: deposit@ccdc.cam.ac.uk.

1 J. S. Miller and A. J. Epstein, in *Progress in Inorganic Chemistry*, S. J. Lippard (Ed.), Wiley: New York, 1975, **20**.
2 J. S. Miller and A. J. Epstein (Eds.), *Synthesis and Properties of Low-Dimensional Materials*, New York Academy of Sciences: New York, 1977, **313**.
3 J. S. Miller (Ed.), *Extended Linear Chain Compounds*, Plenum: New York, 1982.
4 L. Oriol and J. L. Serrano, *Adv. Mater*. 1995, **7**, 348.
5 L. Oriol, in *Metallomesogens*, J. L. Serrano, Ed., VCH: Weinheim, Germany, 1996, 193.
6 L. Oriol, M. Pinol and J. L. Serrano, *Prog. Polym. S*ci., 1997, **22**, 873.
7 G. S. Attard and P. R. Cullum, *Liq. Cryst.,* 1990, **8**, 299.
8 H. D. Burrows and H. A. Ellis, *Thermochim. Acta*, 1982, **52**, 121.
9 H. Abied, D. Guillon, A. Skoulios, P. Weber, A. M. Giroud-Godquin and J. C. Marchon, *Liq. Cryst*., 1987, **2**, 269.
10 G. C. Campbell and J. F. Haw, *Inorg. Chem.,* 1988, **27**, 3706.
11 M. Yamanaka, H. Uekusa, S. Ohba, Y. Saito, S. Iwata, M. Kato, T. Tokii, Y. Muto and O. Steward, *Acta Crystallogr., Sect. B: Struct. Sci.,* 1991, 344.
12 A. Elmali, *Turk. J. Phy*. 2000, **24**, 667.
13 R. Cejudo, G. Alzuet, J. Borrás, M. Liu-González and F. Sanz-Ruiz, *Polyhedron*, 2002, **21**, 1057.
14 N. Abdullah, Y. Al-Hakem, N. Abdullah, H. Samsudin and N. S. A. Tajidi, *Asian J. Chem*., 2014, **26**, 987.
15 R. C. Santra, K. Sengupta, R. Dey, T. Shireen, P. Das, P. S. Guin, K. Mukhopadhyay and S. Das, *J. Coord. Chem*., 2014, **67**, 265.
16 M. Iqbal, I. Ahmad, S. Ali, N. Muhammad, S. Ahmed, M. Sohail. *Polyhedron*, 2013, **50**, 524.
17 M. Kato and Y. Muto, *Inorg. Chem. Rev*., 1988, **92**, 45.
18 L-G. Zhu and S. Kitagawa, *Inorg. Chem. Commun.*, 2003, **6**, 1051.
19 G. M. Sheldrick. SADABS, *Program for Empirical Absorption Correction of Area Detector Data*. University of Göttingen: Göttingen, Germany, 1996.
20 Bruker. APEX2 and SAINT. Bruker AXS Inc., Madison, Wisconsin, USA, 2007.
21 G. M. Sheldrick, *Acta Crystallogr.*, 2008, **A64**, 112.
22 M. Petric, I. Leban and P. Segedin, *Polyhedron*, 1996, **15**, 4277.
23 L. N. Ozair, N. Abdullah and K. M. Lo, Acta Cryst. E67 (2011) 952.
24 K. Nakamoto, *Infrared and Raman Spectra of Inorganic and Coordination Compounds, Applications in Coordination, Organometallic, and Bioinorganic Chemistry*. Wiley-Interscience: 2009.
25 G. B. Deacon and R. J. Phillips, *Coord. Chem. Rev.*, 1980, **33**, 227.
26 X. D. Wang, M. Liang, L. C. Li, Z.H. Jiang, D. Z. Liao, S. P. Yan and P. Cheng, *Struct. Chem*., 2007, **18**, 5.
27 C. Bucher, E. Espinosa, E. Duval, J. –M. Barbe, J. -N. Verpeaux, C. Amatore and R.Guilard. *Eur. J. Inorg. Chem.*, 2001, **4**, 1077.
28 M. Kato, H. B. Jonassen and J. C. Fanning, *Chem. Rev*., 1964, **64**, 99.
29 D. H. Hu, W. Huang, S. H. Gou, J. L. Fang and H. K. Fun, *Polyhedron*, 2003, **22**, 2661.
30 M. I. Mohamadin and N. Abdullah, *Cent. Eur. J. Chem.,* 2010, **8**, 1090.
31 M. F. R. Moita, M. L. T. S. Duarte and R. Fausto, *J. Chem. Soc. Faraday Trans.,* 1994, **90**, 2953.
32 N. Maringa, J. Lenoble, B. Donnio, D. Guillon and R. Deschenaux, *J. Mater. Chem.*, 2008, **18**, 1524.
33 T. Shimogaki, S. Dei, K. Ohta and A. Matsumoto, *J. Mater. Chem.*, 2011, **21**, 10730.
34 Z. Wang, Y. Lan, K. Zhong, Y. Liang, T. Chen, and L. Y. Jin, *Int. J. Mol. Sci.* 2014, **15(4)**, 5634.
35 D. Guillon and A. Skoulios, *J. Phys. IV,* 1996, **C4**, 41.
36 M. Rusjan, B. Donnio, D. Guillon and F. D. Cukiernik, *Chem. Mater.*, 2002, ***14*** **(4)**, 1564.
37 N. Abdullah, N. L. M. Noor, A. R. Nordin, M. A. Halcrow, D. R. MacFarlane, M. A. Lazar, J. M. Pringle, D. W. Bruce, B. Donnio and B. Heinrich, *J. Mater. Chem. C*, 2015, **3**, 2491.
38 S. Mistri, E. Zangrando and S. C. Manna, *Polyhedron*, 2013, **49**, 252.
39 D-B. Dang, M-M. Li, Y. Bai and J-L. Wang, *Spectrochim. Acta Part A*, 2011, **83**, 499.
40 N. P. Cook, V. Torres, D. Jain and A. A. Marti, *J. Am. Chem. Soc*, 2011, **133**, 11121.
41 K. Huang, C. Jiang and A.A. Martin, *Phys. Chem. A*, 2014, **118**, 10353.
42 M. K. Nazeeruddin, A. Kay, I. Rodicio, R. Humpry-Baker, E. Muller, P. Liska, N. Vlachopoulos and M. J. Gratzel, *J. Am. Chem. Soc*., 1993, **115**, 6382.
43 T. J. Kang, S. Fang, M. E. Kozlov, C. S. Haines, N. Li, Y. H. Kim, Y. Chen and R. H. Baughman, *Adv. Funct. Mater.*, 2012, **22**, 477.
44 T. J. Abraham, D. R. MacFarlane and J. M. Pringle, *Energy Environ. Sci.,* 2013, **6**, 2639.
45 T. J. Abraham, D. R. MacFarlane and J. M. Pringle, *Chem. Commun.*, 2011, **47**, 6260.
46 M. Kondo and M. Kubo. *J. Phys. Chem.*, 1958, **62**, 468.
47 J. F. Boas, J. R. Pilbrow and T. D. Smith. *J. Chem. Soc. (A)*, 1969, 721.
48 G. Boschloo and A. Hagfeldt, *Acc. Chem. Res*., 2009, **42**, 1819.

Journal of Materials Chemistry C Accepted Manuscript

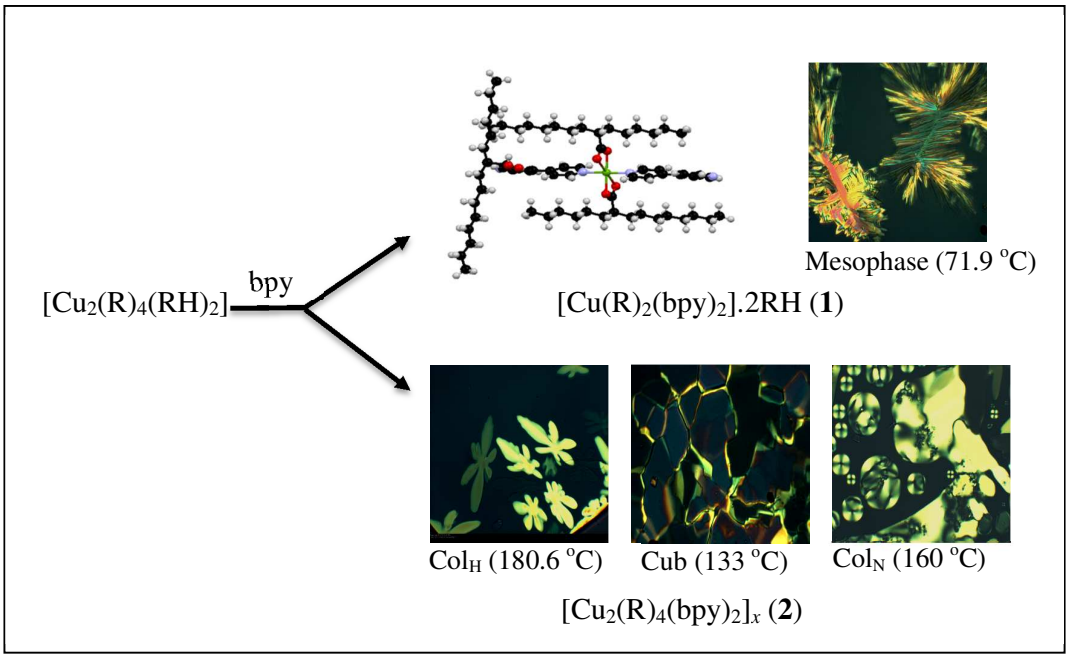

Mononuclear molecular (**1**) and dinuclear polymeric (**2**) complexes of copper(II) with 2-hexyldecanoato (R) and 4,4'-bipyridine (bpy) as ligands exhibited temperature-dependent mesomorphisms

Journal of Materials Chemistry C Accepted Manuscript